

Multi-Instance Partial-Label Learning: Towards Exploiting Dual Inexact Supervision

Wei Tang, Weijia Zhang, and Min-Ling Zhang*

School of Computer Science and Engineering, Southeast University, Nanjing 210096, China
Key Laboratory of Computer Network and Information Integration
(Southeast University), Ministry of Education, China
{tangw, zhangwj, zhangml}@seu.edu.cn

Abstract

Weakly supervised machine learning algorithms are able to learn from ambiguous samples or labels, e.g., multi-instance learning or partial-label learning. However, in some real-world tasks, each training sample is associated with not only multiple instances but also a candidate label set that contains one ground-truth label and some false positive labels. Specifically, at least one instance pertains to the ground-truth label while no instance belongs to the false positive labels. In this paper, we formalize such problems as *multi-instance partial-label learning* (MIPL). Existing multi-instance learning algorithms and partial-label learning algorithms are suboptimal for solving MIPL problems since the former fail to disambiguate a candidate label set, and the latter cannot handle a multi-instance bag. To address these issues, a tailored algorithm named MIPLGP, i.e., *Multi-Instance Partial-Label learning with Gaussian Processes*, is proposed. MIPLGP first assigns each instance with a candidate label set in an augmented label space, then transforms the candidate label set into a logarithmic space to yield the disambiguated and continuous labels via an exclusive disambiguation strategy, and last induces a model based on the Gaussian processes. Experimental results on various datasets validate that MIPLGP is superior to well-established multi-instance learning and partial-label learning algorithms for solving MIPL problems. Our code and datasets will be made publicly available.

*Corresponding author.

1. Introduction

In standard supervised learning, each training sample is represented by a single instance associated with a class label. In recent years, supervised learning has achieved fruitful progress when a large amount of supervision is available. However, annotating large amounts of high-quality labels is time-consuming and costly, especially in fields that require expert knowledge. To overcome these issues, several weakly supervised learning paradigms are proposed and have attracted significant research attention.

According to the quality and number of the labels, weak supervision can be roughly divided into three categories, i.e., incomplete, inexact, and inaccurate supervision [40]. The inexact supervision refers to coarse-grained labels and contains two popular learning frameworks, i.e., multi-instance learning (MIL) and partial-label learning (PLL). As illustrated in Figure 1a, in MIL, multiple training instances are arranged in a bag and we only know the binary bag-level label rather than the instance-level labels [1, 4]. Although the bag-level label is known, the exact labels for the instances in the bag are ambiguous. The framework of PLL is shown in Figure 1b, where each training sample is represented by a single instance coupled with a candidate label set, which consists of a ground-truth label and several false positive labels [13]. Therefore, the mapping from the instance to the concealed ground-truth label is ambiguous. In a sense, multi-instance learning and partial-label learning are dual frameworks to each other in which inexact supervision exists in the instance space and the

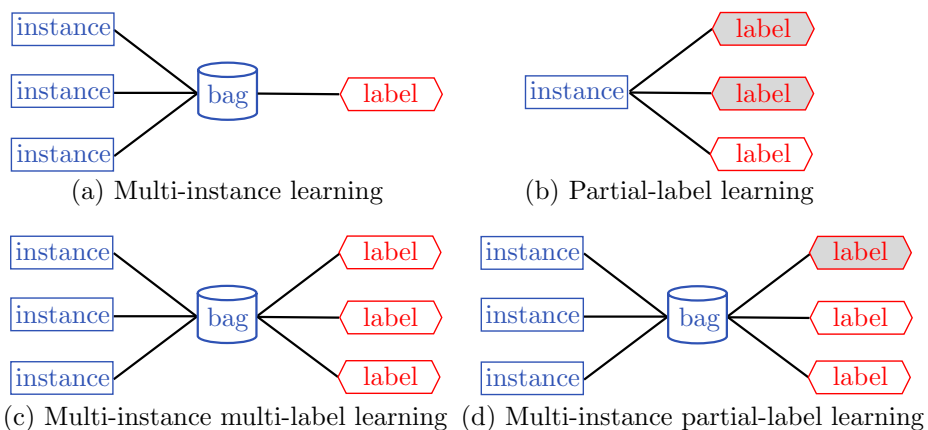


Figure 1: Different weakly supervised learning frameworks, where the grey polygons refer to the false positive labels.

label space, respectively.

However, ambiguities can exist simultaneously in the instance space and the label space. For example, in fine-grained image recognition (as illustrated in Figure 2a), each image can be treated as a multi-instance bag [32]. As the supervision is provided by noisy web labels, the label set of each image contains not only a ground-truth label but also false positive labels [33]. Therefore, we can assign each multi-instance bag with a candidate label set rather than an exact label, and train a model to learn from the partially labeled multi-instance bags. In video classification (as illustrated in Figure 2b), each video consists multiple frames represented as a set of instances, and the labels from social media contain noises that need to be corrected manually [8]. The labeling cost can be significantly reduced if the video classification algorithm can learn from samples represented as sets of instances associated with candidate label sets.

Motivated by the potential applications, we formalize a novel framework named multi-instance partial-label learning (MIPL), which handles ambiguities in the instance space and the label space simultaneously. In Figure 1d, each training sample is represented by a multi-instance bag associated with a bag-level candidate label set, which consists of one ground-truth label and some false positive labels. Moreover, the bag contains at least one instance that belongs to the ground-truth label while no instance pertains to the false positive labels. Therefore, inexact supervision exists both in the instance space and the label space in MIPL. It is noteworthy that multi-instance partial-label learning is different from multi-instance multi-label learning (MIML) presented in Figure 1c, where each multi-instance bag is also associated with a label set [38]. The differences between MIPL and MIML lie in that the label set in MIML only contains ground-truth labels, while the candidate label set in MIPL consists of one ground-truth label and some false positive labels.

To solve the MIPL problems, we propose a tailored algorithm named MIPLGP, i.e., *Multi-Instance Partial-Label learning with Gaussian Processes*. First, in order to assign each instance with a candidate label set containing the ground-truth label, we propose a label augmentation strategy to augment each candidate label set with a negative class label. Second, by virtue of the Dirichlet disambiguation strategy, MIPLGP transforms the augmented

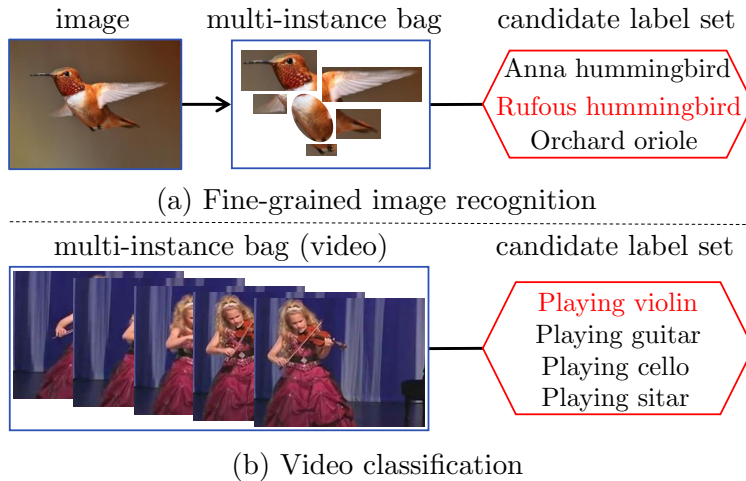


Figure 2: Potential applications of MIPL, where the red is the ground-truth label.

candidate labels to the disambiguated and continuous labels and construct a Gaussian likelihood in a logarithmic space. Last, to infer the parameters of the Dirichlet disambiguation strategy accurately, MIPLGP induces a multi-output Gaussian processes regression model with GPU accelerations.

Empirical evaluation of MIPLGP is conducted on five MIPL datasets. The experimental results indicate that: (a) The MIPL is an exclusive problem that is difficult to be solved by neither multi-instance learning approaches nor partial-label learning approaches. (b) MIPLGP achieves superior results against well-established multi-instance learning and partial-label learning approaches. (c) The proposed label augmentation and Dirichlet disambiguation strategies are both important for solving the MIPL problem.

The rest of the paper is organized as follows. First, related work is briefly reviewed. Second, we present the proposed MIPLGP and report the experimental setting and results. Last, we conclude this paper.

2. Related Work

2.1. Multi-Instance Learning

Multi-instance learning algorithms can be roughly divided into two groups, i.e., instance-level algorithms and bag-level algorithms [1]. The former predict a bag-level label by aggregating

gating instance-level ones, e.g., maximizing or averaging the probabilities of all instances in a bag. The latter induce a classifier by treating each bag as a whole entity, which includes the bag-space paradigm and the embedded-space paradigm.

In general, probabilistic multi-instance methods create a model that characterizes the distribution of instance-level labels and yields aggregated bag-level labels. Kim and la Torre [15] proposes a nonparametric model to capture the underlying generative process by integrating a special bag class likelihood into the Gaussian processes. Along this line, Haußmann *et al.* [10] modifies the standard bag likelihood and infers an instance-label Gaussian processes classifier using variational Bayes. To model the dependencies among the instances, the variational autoencoder is employed to predict both the instance-level and bag-level labels [37, 36]. A recent tendency to address MIL problems is combining neural networks with the attention mechanism, where the attention scores indicate the importance of the instances to the bag [12, 30, 35]. To our knowledge, these MIL methods are designed for binary classification problems, which cannot be directly adopted to solve MIPL problems. Although there are some multi-instance learning algorithms that can handle multi-classification problems [26, 2], they cannot tackle the challenge of false positive labels in the candidate label set.

2.2. Partial-Label Learning

Partial-label learning algorithms utilize identification-based or average-based disambiguation strategies to disambiguate the candidate label sets. The average-based disambiguation strategy treats all labels in the candidate label set equally, and averages the output of the model to achieve disambiguation [5, 9]. The identification-based disambiguation strategy considers the potential ground-truth label as a latent variable, and disambiguates the ambiguous labels by optimizing the objective function related to the latent variable [34, 6].

Based on the graphic model, Jin and Ghahramani [13] minimizes relative entropy between the estimated label distribution and the prior distribution of the class labels. To capture underlying structures of the data, Liu and Dietterich [19] maps training instances to mixture components and samples a label for each mixture component. Based on the Gaussian processes, Zhou *et al.* [39] defines a non-Gaussian likelihood to disambiguate the candidate

label sets and computes the posterior distribution using Laplace approximation. Recently, some deep learning-based disambiguation methods have been investigated for partial-label learning [21, 29]. However, we note that all of them cannot handle multi-instance bags.

3. Methodology

In this section, we propose a MIPL algorithm based on Gaussian processes, i.e., MIPLGP. To the best of our knowledge, this is the first algorithm to address the MIPL problems. First, we introduce the notations and define an augmented label space, which equips each instance among a bag with a suitable candidate label set. Then, we propose a novel Dirichlet disambiguation strategy that effectively disambiguates the candidate label sets. Last, we present a multi-output Gaussian process model.

Let $\mathcal{X} = \mathbb{R}^d$ denote the instance space and $\mathcal{Y} = \{l_1, l_2, \dots, l_q\}$ denote the label space with q class labels. The goal of MIPL is to learn a classifier $h : 2^{\mathcal{X}} \rightarrow \mathcal{Y}$ from a training dataset $\{(\mathbf{X}_i, \mathbf{y}_i) \mid 1 \leq i \leq m\}$ ¹ with m bags and corresponding candidate label sets. Specifically, a multi-instance partial-label sample is denoted as $(\mathbf{X}_i, \mathbf{y}_i)$, where $\mathbf{X}_i = [\mathbf{x}_i^1, \mathbf{x}_i^2, \dots, \mathbf{x}_i^{z_i}]^\top$ is a bag of z_i instances, $\mathbf{x}_i^j \in \mathcal{X}$ for $\forall j \in \{1, 2, \dots, z_i\}$, and $\mathbf{y}_i = [y_i^1, y_i^2, \dots, y_i^q]^\top \in \{0, 1\}^q$ is the candidate label set of \mathbf{X}_i where $y_i^c = 1$ means that the c -th label is one of the candidate labels of \mathbf{X}_i and $y_i^c = 0$ otherwise.

3.1. Label Augmentation

In multi-instance learning, only the bag-level labels are available, while the instance-level labels are unknown. To tackle this problem, a straightforward approach is to propagate the bag label to be the dummy label of all instances in the bag. An obvious problem with this approach is that it will incorrectly assign the negative instances in a positive bag with positive labels. Analogously, in MIPL, if the bag-level candidate label set is directly applied to all the instances in the bag, the ground-truth labels of a substantial amount of

¹Unless otherwise stated, we use symbols in bold to denote matrices and vectors, and use regular symbols to denote scalars.

instances will not exist in their candidate label sets, which violates the settings of partial-label learning.

To address the issue, we propose to utilize an augmented label space $\tilde{\mathcal{Y}} = \{l_1, l_2, \dots, l_q, l_{neg}\}$ with $\tilde{q} = q + 1$ class labels, which augments a negative class label to the original label space \mathcal{Y} . Specifically, we assign instances that do not pertain to label space \mathcal{Y} with the augmented negative class l_{neg} . For example, given a multi-instance bag \mathbf{X}_i associated with a candidate label set $\mathbf{y}_i = [y_i^1, y_i^2, \dots, y_i^q]^\top$, each instance in \mathbf{X}_i is endowed with an augmented candidate label set $\tilde{\mathbf{y}}_i = [y_i^1, y_i^2, \dots, y_i^q, y_i^{neg}]^\top$ where $y_i^{neg} = 1$.

Consequently, we can derive the instance-level features and semantic information based on the augmented label space. Let $\mathbf{X} = [\mathbf{x}_1^1, \mathbf{x}_1^2, \dots, \mathbf{x}_1^{z_1}, \mathbf{x}_2^1, \mathbf{x}_2^2, \dots, \mathbf{x}_m^1, \dots, \mathbf{x}_m^{z_m}]^\top \in \mathbb{R}^{n \times d}$ denote the feature matrix of n instances spread over m bags and $\tilde{\mathbf{Y}} = [\tilde{\mathbf{y}}_1^1, \tilde{\mathbf{y}}_1^2, \dots, \tilde{\mathbf{y}}_1^{z_1}, \tilde{\mathbf{y}}_2^1, \tilde{\mathbf{y}}_2^2, \dots, \tilde{\mathbf{y}}_m^1, \dots, \tilde{\mathbf{y}}_m^{z_m}]^\top \in \mathbb{R}^{n \times \tilde{q}}$ denote the partial-label matrix of the n instances, where $n = \sum_{i=1}^m z_i$ is the total number of the instances in the dataset and $\tilde{\mathbf{y}}_i = \tilde{\mathbf{y}}_i^1 = \tilde{\mathbf{y}}_i^2 = \dots = \tilde{\mathbf{y}}_i^{z_i}$ is the augmented candidate label set of \mathbf{X}_i as well as all instances in bag \mathbf{X}_i . Notably, the label augmentation occurs in the data processing phase, which does not increase training overhead.

3.2. Dirichlet Disambiguation

Motivated by the disambiguation strategies in partial-label learning, we conceive a novel disambiguation strategy for MIPL, which is named *Dirichlet disambiguation*.

Given an augmented MIPL training dataset $(\mathbf{X}, \tilde{\mathbf{Y}})$ with m bags totalling n instances, one instance and its candidate label set can be written as $(\mathbf{x}_i^j, \tilde{\mathbf{y}}_i^j)$ for $\forall i \in \{1, 2, \dots, m\}$ and $j \in \{1, 2, \dots, z_i\}$. When the context is clear, we omit the instance index j to $(\mathbf{x}_i, \tilde{\mathbf{y}}_i)$ for brevity. It is intuitive to use a categorical distribution $\text{Cat}(\boldsymbol{\theta}_i)$ to infer the ground-truth label of the instance, where the class probability $\boldsymbol{\theta}_i = [\theta_i^1, \theta_i^2, \dots, \theta_i^q, \theta_i^{neg}]^\top$ is a multivariate continuous random variable constrained in a q dimensional probability simplex, i.e., $\sum_{c=1}^{\tilde{q}} \theta_i^c = 1$ and $\theta_i^c \geq 0$ ($\forall c \in \{1, 2, \dots, q, neg\}$). It is worth noting that the simplex promotes mutual exclusion among the candidate labels. In order to establish the class probability of the

categorical distribution, we utilize the Dirichlet distribution, which is the conjugate prior to the categorical distribution, to reduce computational difficulty. Accordingly, the Dirichlet distribution $\text{Dir}(\boldsymbol{\alpha}_i)$ with a concentration parameter $\boldsymbol{\alpha}_i = [\alpha_i^1, \alpha_i^2, \dots, \alpha_i^q, \alpha_i^{neg}]^\top$ is adopted to measure $\boldsymbol{\theta}_i$. Concretely, the likelihood model is given by:

$$p(\tilde{\mathbf{y}}_i | \boldsymbol{\alpha}_i) = \text{Cat}(\boldsymbol{\theta}_i), \quad \boldsymbol{\theta}_i \sim \text{Dir}(\boldsymbol{\alpha}_i). \quad (1)$$

To draw the coefficient $\boldsymbol{\theta}_i$ from the Dirichlet distribution, the accurate value of $\boldsymbol{\alpha}_i$ becomes pivotal. In supervised learning, each instance is associated with a unique ground-truth, and thus a constant weight w can be directly added to the index corresponding to the ground-truth. For example, given an observation $\mathbf{y}_i = [y_i^1, y_i^2, \dots, y_i^q]^\top$ that satisfies $y_i^c = 1$ and $y_i^j = 0$ ($\forall j \neq c$), we have $\alpha_i^c = w + \alpha_\epsilon$ and $\alpha_i^j = \alpha_\epsilon$ ($\forall j \neq c$), where α_ϵ is the Dirichlet prior such that $0 < \alpha_\epsilon \ll 1$. However, it is not appropriate to add a constant weight directly in MIPL, since the candidate label set is contaminated by the false positive labels. To overcome this limitation, we propose to synergize the Dirichlet distribution with an iterative disambiguation strategy to identify the ground-truth label from the contaminated candidate label set. To achieve the disambiguation strategy, $\boldsymbol{\alpha}_i = [\alpha_i^1, \alpha_i^2, \dots, \alpha_i^q, \alpha_i^{neg}]$ is initialized with uniform weights for $c \in \{1, 2, \dots, q, neg\}$:

$$\alpha_i^c = \begin{cases} \frac{1}{|\tilde{\mathbf{y}}_i|} + \alpha_\epsilon & \text{if } y_i^c = 1, \\ \alpha_\epsilon & \text{otherwise,} \end{cases} \quad (2)$$

where $0 < \alpha_\epsilon \ll 1$ and $|\tilde{\mathbf{y}}_i|$ is the cardinality which measures the number of non-zero elements in the augmented candidate label set $\tilde{\mathbf{y}}_i$. The softmax value of the classifier output $\tilde{\mathbf{h}}_i = \tilde{\mathbf{h}}(\mathbf{x}_i) = [h_i^1, h_i^2, \dots, h_i^q, h_i^{neg}]^\top$ on the candidate label set indicates the probability that each candidate label is a ground-truth label. Therefore, we utilize the softmax value to gradually eliminate the false positive labels and identify the ground-truth label in each iteration:

$$\alpha_i^c = \begin{cases} \frac{\exp(h_i^c)}{\sum_{y_i^t=1} \exp(h_i^t)} + \alpha_\epsilon & \text{if } y_i^c = 1, \\ \alpha_\epsilon & \text{otherwise.} \end{cases} \quad (3)$$

Next, the problem becomes how to sample from the Dirichlet distribution. Considering both generation quality and cost, we design a two-step process to generate the Dirichlet samples from \tilde{q} independent Gamma-distributed random variables. First, we generate \tilde{q} Gamma-distributed random variables $\{\gamma_i^1, \gamma_i^2, \dots, \gamma_i^q, \gamma_i^{neg}\}$ from the Gamma distribution $\text{Gamma}(\alpha_i^c, 1)$ for $c = 1, 2, \dots, q, neg$, respectively. Then, we normalize the \tilde{q} Gamma-distributed random variables to obtain the realizations. The formulations of the generation process are as follows:

$$\theta_i^c = \frac{\gamma_i^c}{\sum_{j=1}^{\tilde{q}} \gamma_i^j}, \quad \gamma_i^c \sim \text{Gamma}(\alpha_i^c, 1). \quad (4)$$

The probability density function of $\text{Gamma}(\alpha_i^c, 1)$ is $\frac{\gamma^{(\alpha_i^c-1)} \exp(-\gamma)}{\Gamma(\alpha_i^c)}$, where $\alpha_i^c > 0$ is called the shape parameter and $\Gamma(\cdot)$ is the gamma function.

In order to use an exact Gaussian processes model to infer α_i^c accurately, we employ the random variables \dot{x}_i^c drawn from a logarithmic normal distribution $\text{LogNormal}(\dot{y}_i^c, \dot{\sigma}_i^c)$ to approximate the Gamma-distributed random variables γ_i^c by moment matching, i.e., mean matching $\mathbb{E}[\gamma_i^c] = \mathbb{E}[\dot{x}_i^c]$ and variance matching $\mathbb{V}[\gamma_i^c] = \mathbb{V}[\dot{x}_i^c]$:

$$\begin{aligned} \alpha_i^c &= \exp\left(\dot{y}_i^c + \frac{\dot{\sigma}_i^c}{2}\right), \\ \alpha_i^c &= (\exp(\dot{\sigma}_i^c) - 1) \exp(2\dot{y}_i^c + \dot{\sigma}_i^c). \end{aligned} \quad (5)$$

As Milios et al. [23] shows, it is reasonable to estimate γ_i^c by $\text{LogNormal}(\dot{y}_i^c, \dot{\sigma}_i^c)$. The parameters of $\text{LogNormal}(\dot{y}_i^c, \dot{\sigma}_i^c)$ are derived by solving Eq. (5):

$$\begin{aligned} \dot{\sigma}_i^c &= \log\left(\frac{1}{\alpha_i^c} + 1\right), \\ \dot{y}_i^c &= \log \alpha_i^c - \frac{\dot{\sigma}_i^c}{2} = \frac{3}{2} \log \alpha_i^c - \frac{1}{2} \log(\alpha_i^c + 1), \end{aligned} \quad (6)$$

where \dot{y}_i^c is a continuous label in the logarithmic space and $\dot{\sigma}_i^c$ is a variance related to \dot{y}_i^c . Based on the above Dirichlet disambiguation strategy, the original sample $(\mathbf{x}_i, \tilde{\mathbf{y}}_i)$ is transformed into $(\mathbf{x}_i, \dot{\mathbf{y}}_i)$, where $\dot{\mathbf{y}}_i$ is a candidate label set with continuous labels. Meanwhile, a Gaussian likelihood is constructed in the logarithmic space. Given a MIPL training dataset $(\mathbf{X}, \tilde{\mathbf{Y}})$, we reshape the transformed candidate label matrix to yield a row-wise concatenation $\dot{\mathbf{Y}} = [\dot{\mathbf{y}}_1^1; \dot{\mathbf{y}}_1^2; \dots; \dot{\mathbf{y}}_1^{z_1}; \dot{\mathbf{y}}_2^1; \dot{\mathbf{y}}_2^2; \dots; \dot{\mathbf{y}}_m^1, \dots; \dot{\mathbf{y}}_m^{z_m}] \in \mathbb{R}^{\tilde{q}n}$.

3.3. Gaussian Processes Regression Model

Based on the continuous candidate label set matrix $\dot{\mathbf{Y}}$, we can transform the MIPL from a multi-class classification problem to a Gaussian processes regression problem with \tilde{q} outputs. To estimate α_i accurately, we develop a multi-output Gaussian processes regression model for MIPL based on the Gaussian likelihood in the logarithmic space.

For the multi-output Gaussian processes regression model, the vector of \tilde{q} latent functions $\{f^1(\cdot), f^2(\cdot), \dots, f^q(\cdot), f^{neg}(\cdot)\}$ at all n training instances is first introduced: $\mathbf{F} = [\mathbf{f}^1, \mathbf{f}^2, \dots, \mathbf{f}^{neg}]^\top = [f_1^1, \dots, f_n^1, f_1^2, \dots, f_n^2, \dots, f_1^{neg}, \dots, f_n^{neg}]^\top$, where the latent variate \mathbf{F} has length $\tilde{q}n$. The distribution of \mathbf{F} is defined by a prior mean function $\mu = \mathbf{0}$ and a covariance function, i.e., a prior kernel $k(\cdot, \cdot) : \mathbb{R}^d \times \mathbb{R}^d \rightarrow \mathbb{R}$, which is chosen to be a Matérn kernel [24] in this paper. For $\forall c, c' \in \{1, 2, \dots, q, neg\}$, the correlation of the outputs at any a pair of instances \mathbf{x} and \mathbf{x}' can be represented as:

$$\text{Cov}[f^c(\mathbf{x}), f^{c'}(\mathbf{x}')] = k^c(\mathbf{x}, \mathbf{x}') = \begin{cases} \frac{2^{1-\nu}}{\Gamma(\nu)} \left(\frac{\sqrt{2\nu d}}{\ell}\right)^\nu K_\nu\left(\frac{\sqrt{2\nu d}}{\ell}\right) & \text{if } c = c', \\ 0 & \text{otherwise.} \end{cases} \quad (7)$$

Generally speaking, ν is a smoothness parameter and takes the value from $\{0.5, 1.5, 2.5\}$. Here, ℓ is a positive parameter, d is the Euclidean distance between \mathbf{x} and \mathbf{x}' , and K_ν is a modified Bessel function. Finally, the covariance matrix $\mathbf{K} \in \mathbb{R}^{\tilde{q}n \times \tilde{q}n}$ of the \tilde{q} latent processes is block diagonal by the matrices $\mathbf{K}^1, \mathbf{K}^2, \dots, \mathbf{K}^{\tilde{q}}$ of shape $n \times n$. Gaussian processes place a Gaussian prior over latent variable $\mathbf{F} \sim \mathcal{GP}(\mathbf{0}, \mathbf{K})$, i.e., $P(\mathbf{F} | \mathbf{X}) = \mathcal{N}(\mathbf{0}, \mathbf{K})$, and the Gaussian likelihood in the logarithmic space is $P(\dot{\mathbf{Y}} | \mathbf{F}) = \mathcal{N}(\mathbf{F}, \Sigma)$, where Σ is the matrix form of $\dot{\sigma}_i^c$ in $\text{LogNormal}(\dot{y}_i^c, \dot{\sigma}_i^c)$. Following the Bayes' rule, the posterior distribution $P(\mathbf{F} | \mathbf{X}, \dot{\mathbf{Y}}) \propto P(\mathbf{F} | \mathbf{X})P(\dot{\mathbf{Y}} | \mathbf{F})$ and the marginal likelihood $P(\dot{\mathbf{Y}} | \mathbf{X}) = \int_{\mathbf{F}} P(\mathbf{F} | \mathbf{X})P(\dot{\mathbf{Y}} | \mathbf{F})$ are both Gaussian.

The above likelihoods are based on the instances-level features and labels. In multi-instance learning, however, a ubiquitous issue is how to aggregate the instance labels to generate a bag label. This problem also takes place in MIPL and is more difficult due to the ambiguous multi-class classification. A feasible solution is to set the bag label with the class label corresponding to the maximum value among the class probabilities of all instances in the

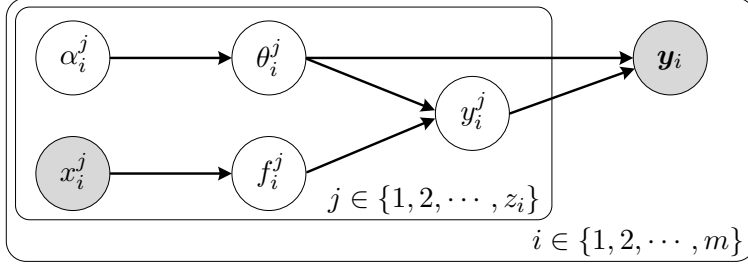


Figure 3: Plate diagram for MIPLGP, where the grey circles and white ones are the observed variables and latent variables, respectively.

bag. Let $\tilde{\Theta}_i = [\theta_i^1, \theta_i^2, \dots, \theta_i^{z_i}]^\top \in \mathbb{R}^{z_i \times \tilde{q}}$ ($\theta_i^j = [\theta_i^1, \theta_i^2, \dots, \theta_i^q, \theta_i^{neg}]^\top$ for $j = 1, 2, \dots, z_i$) denote the class probabilities of the multi-instance bag \mathbf{X}_i among \tilde{q} outputs. We truncate $\tilde{\Theta}_i$ to yield $\Theta_i = [\hat{\theta}_i^1, \hat{\theta}_i^2, \dots, \hat{\theta}_i^{z_i}]^\top \in \mathbb{R}^{z_i \times q}$ among q outputs, where $\hat{\theta}_i^j = [\theta_i^1, \theta_i^2, \dots, \theta_i^q]^\top$. Consequently, the aggregated bag label is as follows:

$$Y_i = \psi(\Theta_i), \quad (8)$$

where the goal of $\psi(\Theta_i)$ is to query the column index corresponding to the maximum value in Θ_i . The plate diagram of MIPLGP is illustrated in Figure 3, where the grey circles represent the observed variables, i.e., features and bag labels, and the white circles represent the latent variables.

In the training phase, the model parameters Φ are learned by minimizing the negative log marginal likelihood:

$$\mathcal{L} = -\log P(\dot{\mathbf{Y}} | \mathbf{X}, \Phi) \propto \log |\mathbf{K}| + \dot{\mathbf{Y}}^\top \mathbf{K}^{-1} \dot{\mathbf{Y}}, \quad (9)$$

and the derivative is as follows:

$$\frac{\partial \mathcal{L}}{\partial \Phi} \propto \text{Tr} \left(\mathbf{K}^{-1} \frac{\partial \mathbf{K}}{\partial \Phi} \right) - \dot{\mathbf{Y}}^\top \mathbf{K} \frac{\partial \mathbf{K}^{-1}}{\partial \Phi} \mathbf{K} \dot{\mathbf{Y}}, \quad (10)$$

where $\text{Tr}(\cdot)$ is the trace operation. In a naive GP, the Cholesky decomposition of \mathbf{K}^{-1} requires $\mathcal{O}(\tilde{q}n^3)$ computations. However, we employ an efficient algorithm with GPU accelerations and reduce the complexity to $\mathcal{O}(\tilde{q}n^2)$. Moreover, a preconditioner is adopted to further accelerate the computation [27].

Given an unseen multi-instance bag $\mathbf{X}_* = [\mathbf{x}^1, \mathbf{x}^2, \dots, \mathbf{x}^{z_*}]$ with z_* instances, the GP model generates the predictive distribution $P(\mathbf{F}^* | \mathbf{X}, \dot{\mathbf{Y}}, \mathbf{x}^{i_*})$ ($i_* = 1, 2, \dots, z_*$) for the corresponding latent variables $\mathbf{F}^* = [f^{*1}, f^{*2}, \dots, f^{*\bar{q}}]^\top$. The Dirichlet posterior of the class label is procured from the predictive distribution using the Monte Carlo method so as to calculate the expectation of class probability:

$$\mathbb{E}[\theta_{i_*}^c | \mathbf{X}, \dot{\mathbf{Y}}, \mathbf{x}^{i_*}] = \int_{\mathbf{F}^*} \frac{\exp(f^{*c}(\mathbf{x}^{i_*}))}{\sum_{j=1}^{\bar{q}} \exp(f^{*j}(\mathbf{x}^{i_*}))} P(f^{*c}(\mathbf{x}^{i_*}) | \mathbf{X}, \dot{\mathbf{Y}}, \mathbf{x}^{i_*}), \quad (11)$$

where $P(f^{*c}(\mathbf{x}^{i_*}) | \mathbf{X}, \dot{\mathbf{Y}}, \mathbf{x}^{i_*})$ is the predictive distribution for $f^{*c}(\cdot, \cdot)$. We write the class probability of \mathbf{x}^{i_*} as $\boldsymbol{\theta}_{i_*}^{i_*} = [\theta_{i_*}^1, \theta_{i_*}^2, \dots, \theta_{i_*}^q, \theta_{i_*}^{neg}]$, and let $\tilde{\boldsymbol{\Theta}}_* = [\boldsymbol{\theta}_*^1, \boldsymbol{\theta}_*^2, \dots, \boldsymbol{\theta}_*^{z_*}]^\top \in \mathbb{R}^{z_* \times \bar{q}}$ denote the class probabilities of all instances in the test bag \mathbf{X}_* . Then, we consider the label space \mathcal{Y} instead of $\tilde{\mathcal{Y}}$, i.e., remove the probabilities corresponding to class l_{neg} and get $\boldsymbol{\Theta}_* \in \mathbb{R}^{z_* \times q}$ with z_* instances and q class labels. Finally, a bag label is predicted by:

$$Y_* = \psi(\boldsymbol{\Theta}_*). \quad (12)$$

Algorithm 1 summarizes the complete procedure of MIPLGP. First, the algorithm propagates the augmented candidate label set of each bag to all instances in the bag (Steps 1-7). After initializing the shape parameter of the Dirichlet distribution (Step 8), the Gaussian processes model is induced based on the transformed labels (Steps 9-21). Last, the label of an unseen multi-instance bag is returned by querying the predicted class probabilities (Step 22).

4. Experiments

4.1. Experimental Setup

4.1.1. Datasets

To the best of our knowledge, there are no ready-made datasets for solving the MIPL problems. To overcome this limitation, we synthesize five MIPL datasets stemming from

Algorithm 1 $Y_* = \text{MIPLGP}(\mathcal{D}, \alpha_\epsilon, T, \mathbf{X}_*)$

Inputs:

\mathcal{D} : the multi-instance partial-label training set $\{(\mathbf{X}_i, \mathbf{y}_i) \mid 1 \leq i \leq m\}$ ($\mathbf{X}_i = [\mathbf{x}_i^1, \mathbf{x}_i^2, \dots, \mathbf{x}_i^{z_i}]^\top$, $\mathbf{x}_i^{z_i} \in \mathcal{X}$, $\mathbf{X}_i \subseteq \mathcal{X}$, $\mathcal{X} = \mathbb{R}^d$, $\mathbf{y}_i = [y_i^1, y_i^2, \dots, y_i^q]^\top$, $\mathbf{y}_i \subseteq \mathcal{Y}$, $\mathcal{Y} = \{l_1, l_2, \dots, l_q\}$)

α_ϵ : the Dirichlet prior

T : the number of iterations

\mathbf{X}_* : the unseen multi-instance bags with z_* instances

Outputs:

Y_* : the predicted bag label for \mathbf{X}_*

Process:

- 1: Augment \mathcal{Y} to $\tilde{\mathcal{Y}} = \{l_1, l_2, \dots, l_q, l_{neg}\}$
 - 2: **for** $i = 1$ to m **do**
 - 3: Augment \mathbf{y}_i to $\tilde{\mathbf{y}}_i = [y_i^1, y_i^2, \dots, y_i^q, y_i^{neg}]^\top$
 - 4: **for** $j = 1$ to z_i **do**
 - 5: Propagate $\tilde{\mathbf{y}}_i$ to be the label of each instance \mathbf{x}_i^j
 - 6: **end for**
 - 7: **end for**
 - 8: Initialize α_i as defined in Eq. (2)
 - 9: **for** $t = 1$ to T **do**
 - 10: **for** $i = 1$ to m **do**
 - 11: **for** $j = 1$ to z_i **do**
 - 12: Model the likelihood $p(\tilde{\mathbf{y}}_i \mid \alpha_i) = \text{Cat}(\theta_i)$, $\theta_i \sim \text{Dir}(\alpha_i)$ according to Eq. (1)
 - 13: Generate Dirichlet samples from the Gamma distribution according to Eq. (4)
 - 14: Derive the continuous candidate label set $\hat{\mathbf{y}}_i$ as stated by Eq. (6)
 - 15: **end for**
 - 16: **end for**
 - 17: Calculate \mathcal{L} according to Eq. (9)
 - 18: Calculate gradient $\frac{\partial \mathcal{L}}{\partial \Phi}$ as defined in Eq. (10)
 - 19: Update Φ by the optimizer
 - 20: Update α_i according to Eq. (3)
 - 21: **end for**
 - 22: Return Y_* according to Eq. (12)
-

relevant literature [18, 31, 17, 3, 25], i.e., MNIST-MIPL, FMNIST-MIPL, Newsgroups-MIPL, Birdsong-MIPL, and SIVAL-MIPL, from domains of image, text, and biology to compare MIPLGP with other algorithms.

The characteristics of the synthetic datasets are summarized in Table 1. We use *#bags*, *#ins*, *#max*, *#min*, *#dims*, *#l-o*, *#l-t*, *#l-r*, and *percentage* to denote the number of bags, number of instances, maximum number of instances in a bag, minimum number of instances in a bag, dimension of each instance, number of targeted class labels in the corresponding

Table 1: Characteristics of the MIPL Datasets.

Dataset	#bags	#ins	#max	#min	#dims	#l-o	#l-t	#l-r	percentage	domain
MNIST-MIPL	500	20664	48	35	784	10	5	5	8.0%	image
FMNIST-MIPL	500	20810	48	36	784	10	5	5	8.0%	image
Newsgroups-MIPL	1000	43122	86	11	200	20	10	10	8.0%	text
Birdsong-MIPL	1300	48425	76	25	38	13	13	1	8.3%	biology
SIVAL-MIPL	1500	47414	32	31	30	25	25	-	25.6%	image

literature, number of targeted class labels in MIPL, number of reserved class labels, and percentage of the number of positive instances in each dataset.

To synthesize the multi-instance bag with a candidate label set, we take positive instances of the corresponding label from the targeted class labels and negative instances in the whole reserved class labels. Furthermore, we sample the false positive labels from the target classes without replacement. For comprehensive performance evaluation, the number of false positive labels depends on the controlling parameter r ($|\mathbf{y}_i| = r + 1$). Note that we sample all instances and generate false positive labels randomly and uniformly.

Take MNIST-MIPL for example, the number of MNIST is 10 in most classification problems. To obtain a multi-instance bag in the MIPL, we extract $\{0, 2, 4, 6, 8\}$ as five target classes for providing the positive instances according to the corresponding class and draw all negative ones from the reserved classes $\{1, 3, 5, 7, 9\}$ randomly. Then, we append any r false positive labels from the target classes to the candidate label set of the multi-instance bag. More detailed information on the MIPL datasets is provided in Appendix A.

4.1.2. Comparative Algorithms

MIPLGP is compared against four well-established multi-instances learning algorithms including three Gaussian processes-based algorithms VWSGP [14], VGPMIL [10], and LM-VGPMIL [10], as well as variational autoencoder based algorithm MIVAE [37]. In addition, we employ six partial-label learning algorithms containing two averaging-based algorithms PL-KNN [11] and CLPL [5], two identification-based algorithms LSB-CMM [19] and SURE [6], graph matching based disambiguation algorithm GM-PLL [22], and feature-aware disambiguation algorithm PL-AGGD [28]. The parameter configurations of each algorithm are suggested in the respective literature.

To verify the effectiveness of the Dirichlet disambiguation and the label augmentation, we evaluate two variants of MIPLGP, i.e., MIPLGP-uniform and MIPLGP-naive. The former utilizes the uniform weights as defined in Eq. (2) throughout the iterations, and the latter handles the candidate label sets only in the original label space \mathcal{Y} .

4.1.3. Implementation

We implement MIPLGP using GPyTorch, which is a modular Gaussian process library in PyTorch [7]. For MIPLGP and its variants, we use the Adam optimizer [16] with $\beta_1 = 0.9$ and $\beta_2 = 0.999$. The initial learning rate is 0.1 which is decayed via a cosine annealing method [20]. We set the number of iterations to 500 for MNIST-MIPL and FMNIST-MIPL datasets and 50 for the remaining three datasets. For Newsgroups-MIPL dataset, the smoothness parameter ν in Matérn kernel is 0.5, while $\nu = 2.5$ for the rest. We uniform that ℓ in Matérn kernel is equal to 1, $\alpha_\epsilon = 0.0001$, the size of the preconditioner is 100, and the number of Monte Carlo sampling points is 512 for all datasets. We perform ten runs of 50%/50% random train/test splits on all datasets, and record the mean accuracies and standard deviations for each algorithm. Specifically, we conduct the pairwise t-test at a 0.05 significance level based on the results of ten runs. Experiments are mainly conducted with two Nvidia Tesla V100 GPUs.

4.2. Experimental Results

Since multi-instance learning and partial-label learning are both special cases of MIPL, we carry out experiments with multi-instance learning and partial-label learning algorithms using different versions of degenerated MIPL datasets. However, the experiments with MIPLGP and its variants are executed on the standard MIPL datasets.

4.2.1. Comparison with Partial Learning Algorithms

Existing partial-label learning algorithms are incapable of handling the multi-instance bag. Therefore, an aggregated feature representation of the bag is a prerequisite for tackling the

MIPL problems with partial-label learning algorithms. In multi-instance learning, the idea of the embedded-space paradigm is to explicitly distill the whole bag by defining a mapping function from the bag to a feature vector. Inspired by the idea, we utilize two schemes to map the bag to a holistic feature vector, respectively.

- **Mean** scheme: For each bag, the average value of all instances in the corresponding feature dimension is calculated as the final feature value in that dimension. The dimension of the holistic feature vector is the same as that of each instance.
- **MaxMin** scheme: We choose the maximum values of all instances in each feature dimension and concatenate them with the minimum values of all instances in each feature dimension. Finally, the holistic feature representation of a bag is distilled with the length of $2d$.

The classification results with the varying number of false positive labels r are reported in Table 2, and Table 3 summarizes the win/tie/loss counts between MIPLGP and each comparing algorithm. MIPLGP achieves superior or competitive performance against the comparing algorithms. Out of the 180 statistical tests, we yield the following observations:

- MIPLGP is statistically superior to the comparing partial-label learning algorithms in 99.444% of the cases.
- Compared to MIPLGP-uniform and MIPLGP-naive, MIPLGP achieves statistically favorable performance in 86.667% and 93.333% of the cases, respectively.
- Regardless of the Mean scheme or MaxMin scheme, MIPLGP consistently outperforms the comparing partial-label learning algorithms by a notable margin, e.g., more than 5.3 percent, in almost all cases.
- In most cases, MIPLGP-uniform is superior to MIPLGP-naive, which means that the label augmentation strategy plays an important role in MIPLGP. As the average accuracy of MIPLGP-uniform decreases faster than that of MIPLGP-naive as the number of false positive labels increases, the results demonstrate that the Dirichlet disambiguation is indispensable especially when there are a lot of false positive labels.

Table 2: Classification accuracy (mean \pm std) of each comparing algorithm in terms of the different number of false positive candidate labels [$r \in \{1, 2, 3\}$]. \bullet/\circ indicates whether the performance of MIPLGP is statistically superior/inferior to the comparing algorithm on each dataset (pairwise t-test at 0.05 significance level).

Algorithm	r	MNIST-MIPL	FMNIST-MIPL	Newsgroups-MIPL	Birdsong-MIPL	SIVAL-MIPL
MIPLGP	1	0.921 \pm 0.018	0.806 \pm 0.031	0.432 \pm 0.018	0.628 \pm 0.012	0.599 \pm 0.020
	2	0.712 \pm 0.045	0.778 \pm 0.042	0.424 \pm 0.019	0.589 \pm 0.020	0.535 \pm 0.020
	3	0.521 \pm 0.084	0.592 \pm 0.076	0.373 \pm 0.023	0.538 \pm 0.014	0.497 \pm 0.023
MIPLGP-uniform	1	0.834 \pm 0.023 \bullet	0.778 \pm 0.031 \bullet	0.417 \pm 0.019 \bullet	0.623 \pm 0.013 \bullet	0.595 \pm 0.023
	2	0.531 \pm 0.070 \bullet	0.746 \pm 0.042 \bullet	0.401 \pm 0.025 \bullet	0.581 \pm 0.022 \bullet	0.530 \pm 0.019 \bullet
	3	0.206 \pm 0.009 \bullet	0.226 \pm 0.039 \bullet	0.365 \pm 0.013	0.526 \pm 0.016 \bullet	0.489 \pm 0.026 \bullet
MIPLGP-naive	1	0.522 \pm 0.025 \bullet	0.570 \pm 0.016 \bullet	0.422 \pm 0.019 \bullet	0.551 \pm 0.010 \bullet	0.585 \pm 0.019 \bullet
	2	0.438 \pm 0.049 \bullet	0.468 \pm 0.065 \bullet	0.407 \pm 0.025 \bullet	0.511 \pm 0.026 \bullet	0.523 \pm 0.018 \bullet
	3	0.309 \pm 0.072 \bullet	0.258 \pm 0.045 \bullet	0.373 \pm 0.017	0.464 \pm 0.019 \bullet	0.480 \pm 0.021 \bullet
Mean						
PL-kNN	1	0.397 \pm 0.021 \bullet	0.419 \pm 0.032 \bullet	0.133 \pm 0.009 \bullet	0.213 \pm 0.011 \bullet	0.155 \pm 0.009 \bullet
	2	0.337 \pm 0.020 \bullet	0.360 \pm 0.030 \bullet	0.148 \pm 0.006 \bullet	0.197 \pm 0.012 \bullet	0.138 \pm 0.008 \bullet
	3	0.284 \pm 0.023 \bullet	0.264 \pm 0.032 \bullet	0.142 \pm 0.010 \bullet	0.182 \pm 0.009 \bullet	0.123 \pm 0.009 \bullet
CLPL	1	0.644 \pm 0.023 \bullet	0.734 \pm 0.031 \bullet	0.131 \pm 0.027 \bullet	0.330 \pm 0.013 \bullet	0.239 \pm 0.009 \bullet
	2	0.528 \pm 0.033 \bullet	0.671 \pm 0.023 \bullet	0.112 \pm 0.015 \bullet	0.295 \pm 0.012 \bullet	0.221 \pm 0.012 \bullet
	3	0.377 \pm 0.042 \bullet	0.524 \pm 0.046	0.111 \pm 0.012 \bullet	0.282 \pm 0.011 \bullet	0.200 \pm 0.017 \bullet
LSB-CMM	1	0.631 \pm 0.045 \bullet	0.709 \pm 0.025 \bullet	0.100 \pm 0.000 \bullet	0.260 \pm 0.013 \bullet	0.144 \pm 0.012 \bullet
	2	0.416 \pm 0.047 \bullet	0.560 \pm 0.059 \bullet	0.100 \pm 0.000 \bullet	0.242 \pm 0.013 \bullet	0.116 \pm 0.014 \bullet
	3	0.277 \pm 0.038 \bullet	0.295 \pm 0.032 \bullet	0.100 \pm 0.000 \bullet	0.218 \pm 0.011 \bullet	0.095 \pm 0.015 \bullet
SURE	1	0.666 \pm 0.027 \bullet	0.753 \pm 0.019 \bullet	0.358 \pm 0.019 \bullet	0.345 \pm 0.008 \bullet	0.313 \pm 0.022 \bullet
	2	0.512 \pm 0.031 \bullet	0.685 \pm 0.013 \bullet	0.300 \pm 0.013 \bullet	0.319 \pm 0.008 \bullet	0.284 \pm 0.019 \bullet
	3	0.344 \pm 0.075 \bullet	0.441 \pm 0.063 \bullet	0.251 \pm 0.017 \bullet	0.308 \pm 0.013 \bullet	0.256 \pm 0.013 \bullet
GM-PLL	1	0.248 \pm 0.014 \bullet	0.268 \pm 0.030 \bullet	0.183 \pm 0.012 \bullet	0.146 \pm 0.018 \bullet	0.175 \pm 0.013 \bullet
	2	0.260 \pm 0.022 \bullet	0.251 \pm 0.019 \bullet	0.180 \pm 0.015 \bullet	0.106 \pm 0.012 \bullet	0.160 \pm 0.014 \bullet
	3	0.235 \pm 0.028 \bullet	0.246 \pm 0.021 \bullet	0.157 \pm 0.015 \bullet	0.092 \pm 0.012 \bullet	0.136 \pm 0.013 \bullet
PL-AGGD	1	0.643 \pm 0.021 \bullet	0.714 \pm 0.017 \bullet	0.325 \pm 0.009 \bullet	0.332 \pm 0.010 \bullet	0.312 \pm 0.023 \bullet
	2	0.535 \pm 0.034 \bullet	0.642 \pm 0.026 \bullet	0.256 \pm 0.015 \bullet	0.304 \pm 0.013 \bullet	0.277 \pm 0.019 \bullet
	3	0.363 \pm 0.039 \bullet	0.429 \pm 0.040 \bullet	0.213 \pm 0.015 \bullet	0.292 \pm 0.015 \bullet	0.244 \pm 0.011 \bullet
MaxMin						
PL-kNN	1	0.388 \pm 0.023 \bullet	0.309 \pm 0.029 \bullet	0.119 \pm 0.004 \bullet	0.274 \pm 0.009 \bullet	0.177 \pm 0.007 \bullet
	2	0.330 \pm 0.016 \bullet	0.288 \pm 0.019 \bullet	0.135 \pm 0.008 \bullet	0.270 \pm 0.006 \bullet	0.153 \pm 0.009 \bullet
	3	0.266 \pm 0.025 \bullet	0.239 \pm 0.021 \bullet	0.138 \pm 0.007 \bullet	0.250 \pm 0.011 \bullet	0.136 \pm 0.011 \bullet
CLPL	1	0.481 \pm 0.020 \bullet	0.364 \pm 0.026 \bullet	0.246 \pm 0.009 \bullet	0.361 \pm 0.016 \bullet	0.266 \pm 0.011 \bullet
	2	0.396 \pm 0.028 \bullet	0.332 \pm 0.021 \bullet	0.200 \pm 0.009 \bullet	0.328 \pm 0.014 \bullet	0.223 \pm 0.010 \bullet
	3	0.334 \pm 0.039 \bullet	0.332 \pm 0.028 \bullet	0.166 \pm 0.018 \bullet	0.300 \pm 0.015 \bullet	0.199 \pm 0.014 \bullet
LSB-CMM	1	0.372 \pm 0.099 \bullet	0.238 \pm 0.073 \bullet	0.221 \pm 0.018 \bullet	0.319 \pm 0.011 \bullet	0.248 \pm 0.015 \bullet
	2	0.324 \pm 0.038 \bullet	0.284 \pm 0.039 \bullet	0.146 \pm 0.039 \bullet	0.292 \pm 0.014 \bullet	0.200 \pm 0.017 \bullet
	3	0.220 \pm 0.017 \bullet	0.210 \pm 0.017 \bullet	0.113 \pm 0.021 \bullet	0.272 \pm 0.020 \bullet	0.157 \pm 0.017 \bullet
SURE	1	0.528 \pm 0.021 \bullet	0.404 \pm 0.023 \bullet	0.316 \pm 0.015 \bullet	0.381 \pm 0.013 \bullet	0.372 \pm 0.022 \bullet
	2	0.415 \pm 0.028 \bullet	0.351 \pm 0.025 \bullet	0.274 \pm 0.013 \bullet	0.371 \pm 0.015 \bullet	0.324 \pm 0.013 \bullet
	3	0.321 \pm 0.030 \bullet	0.304 \pm 0.029 \bullet	0.245 \pm 0.014 \bullet	0.341 \pm 0.014 \bullet	0.288 \pm 0.011 \bullet
GM-PLL	1	0.386 \pm 0.024 \bullet	0.195 \pm 0.016 \bullet	0.209 \pm 0.020 \bullet	0.180 \pm 0.019 \bullet	0.143 \pm 0.013 \bullet
	2	0.346 \pm 0.030 \bullet	0.225 \pm 0.019 \bullet	0.181 \pm 0.018 \bullet	0.139 \pm 0.023 \bullet	0.121 \pm 0.014 \bullet
	3	0.294 \pm 0.024 \bullet	0.221 \pm 0.013 \bullet	0.163 \pm 0.019 \bullet	0.121 \pm 0.020 \bullet	0.104 \pm 0.012 \bullet
PL-AGGD	1	0.514 \pm 0.024 \bullet	0.392 \pm 0.016 \bullet	0.289 \pm 0.014 \bullet	0.370 \pm 0.013 \bullet	0.361 \pm 0.021 \bullet
	2	0.428 \pm 0.035 \bullet	0.346 \pm 0.019 \bullet	0.249 \pm 0.013 \bullet	0.353 \pm 0.014 \bullet	0.310 \pm 0.013 \bullet
	3	0.333 \pm 0.039 \bullet	0.324 \pm 0.025 \bullet	0.212 \pm 0.011 \bullet	0.328 \pm 0.015 \bullet	0.277 \pm 0.013 \bullet

4.2.2. Comparison with Multi-Instance Learning Algorithms

Most of the existing multi-instance learning algorithms are only designed to solve binary classification problems, and thus are not directly applicable to the MIPL problems.

	MIPLGP against						In total
	PL-kNN	CLPL	LSB-CMM	SURE	GM-PLL	PL-AGGD	
$r = 1$	10/0/0	10/0/0	10/0/0	10/0/0	10/0/0	10/0/0	60/0/0
$r = 2$	10/0/0	10/0/0	10/0/0	10/0/0	10/0/0	10/0/0	60/0/0
$r = 3$	10/0/0	9/1/0	10/0/0	10/0/0	10/0/0	10/0/0	59/1/0
In total	30/0/0	29/1/0	30/0/0	30/0/0	30/0/0	30/0/0	179/1/0

Table 3: Win/tie/loss counts on the classification performance of MIPLGP against the comparing PLL algorithms.

To make multi-instance learning algorithms fit the MIPL problems, we employ the *One vs. Rest (OvR)* decomposition strategy. Specifically, given a multi-instance bag \mathbf{X}_i associated with a candidate label set \mathbf{y}_i , we assign each label in the candidate label set to the bag in turn and yield $|\mathbf{y}_i|$ multi-instance bags with a single bag-level label. For $c = 1, 2, \dots, q$, we recompose the label c to 1, i.e., positive, and other labels to 0, i.e., negative. After recomposing all multi-instance bags for the label c , we train and test the c -th classifier. For an unseen multi-instance bag, we can obtain q predictions from the q classifiers. If only one of the predictions is positive, the corresponding class label of the positive prediction is regarded as the classification result of the bag. If the number of positive predictions among the q predictions is greater than one, the class label corresponding to the classifier with the largest prediction confidence is selected as the classification result of the bag. If the predictions of q classifiers all are negative, the classification result is the class label with the lowest prediction confidence.

The computational cost of multi-instance learning algorithms rises with the increase of false positive labels, and the classification accuracy decreases accordingly. We present the classification accuracy of multi-instance learning algorithms with one false positive label in

Table 4: Classification accuracy (mean \pm std) of each comparing algorithm (with one false positive candidate label [$r = 1$]). \bullet/\circ indicates whether the performance of MIPLGP is statistically superior/inferior to the comparing algorithm on each dataset (pairwise t-test at 0.05 significance level).

Algorithm	MNIST-MIPL	FMNIST-MIPL	Newsgroups-MIPL	Birdsong-MIPL	SIVAL-MIPL
MIPLGP	0.921 \pm 0.018	0.806 \pm 0.031	0.432 \pm 0.018	0.628 \pm 0.012	0.599 \pm 0.020
VWSGP	0.402 \pm 0.026 \bullet	0.422 \pm 0.028 \bullet	0.098 \pm 0.013 \bullet	0.250 \pm 0.047 \bullet	0.050 \pm 0.009 \bullet
VGPMIL	0.469 \pm 0.047 \bullet	0.455 \pm 0.034 \bullet	0.097 \pm 0.010 \bullet	0.080 \pm 0.034 \bullet	0.041 \pm 0.006 \bullet
LM-VGPMIL	0.471 \pm 0.021 \bullet	0.486 \pm 0.036 \bullet	0.101 \pm 0.008 \bullet	0.081 \pm 0.042 \bullet	0.045 \pm 0.008 \bullet
MIVAE	0.793 \pm 0.019 \bullet	0.638 \pm 0.213	0.135 \pm 0.245 \bullet	0.067 \pm 0.091 \bullet	0.068 \pm 0.119 \bullet

Table 4, which reveals that:

- MIPLGP achieves significantly better performances against the comparing multi-instance learning algorithms in almost all cases.
- Due to the noisy bag-level labels in the degenerated datasets, the comparing multi-instance learning algorithms can learn well in multi-instance learning but cannot effectively work on the MIPL datasets, such as Newsgroups-MIPL, Birdsong-MIPL, and SIVAL-MIPL. This phenomenon indicates that it is necessary to propose tailored algorithms for solving the MIPL problems effectively.

4.3. Further Analyses

4.3.1. Exploration of Dirichlet Prior α_ϵ

As defined in Eqs. (2), (3), and (6), the transformed labels are affected by the Dirichlet prior α_ϵ . When α_ϵ approaches 0, the transformed labels and variances of non-candidate labels become negative infinity and positive infinity, respectively, which makes the Gaussian processes regression impossible. To avoid this issue, the Dirichlet prior plays a role in restricting the transformed labels of the non-candidate labels finite. At the same time, the consequential labels and variances of candidate labels are negative values and positive ones that come near to 0. During the iterations, the transformed results of the ground-truth labels are closer to 0 than those of the false positive labels, and the differences between the ground-truth labels and the false positive ones become larger.

The classification accuracy of MIPLGP with the varying number false positive labels $r \in \{1, 2, 3, 4, 5\}$ and the different Dirichlet prior $\alpha_\epsilon \in \{0.0001, 0.001, 0.01\}$ on the MIPL datasets is shown in Figure 4. There are several observations:

- On MNIST-MIPL and Newsgroups-MIPL datasets, the smaller α_ϵ can achieve better results, while the results are reversed on SIVAL-MIPL dataset.

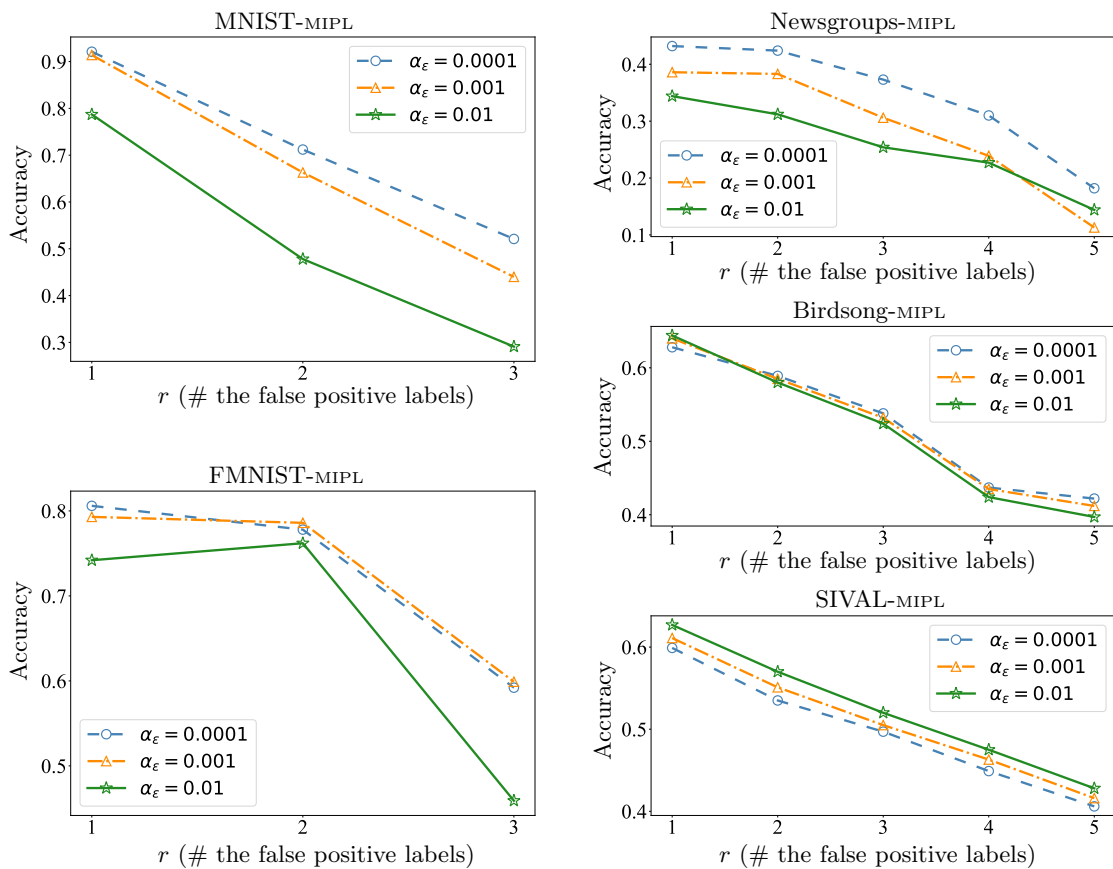


Figure 4: Classification accuracy of MIPLGP on the MIPL datasets with varying r and α_ϵ .

- On Birdsong-MIPL datasets, the differences between the varying α_ϵ are slight. Similarly, there is no obvious difference between the $\alpha_\epsilon = 0.0001$ and $\alpha_\epsilon = 0.001$ on FMNIST-MIPL dataset.
- Different datasets have diverse optimums of the Dirichlet prior, which are determined by the characteristics of the datasets themselves.

In our experiments on MIPLGP and the two variants, we set α_ϵ to 0.0001 which can perform satisfactorily on all datasets.

5. Conclusion

In this paper, we formalize a novel learning framework named multi-instance partial-label learning (MIPL), where each training sample is associated with not only multiple instances but also a candidate label set that contains one ground-truth label and some false positive labels. Although the MIPL problems widely exist in many real-world applications, to the best of our knowledge, MIPLGP proposed in this paper is the first tailored MIPL algorithm. Specifically, MIPLGP transforms the candidate label sets from the augmented label space into a logarithmic space, yielding a Gaussian likelihood and transforming the classification problem into a regression problem. To solve the regression problem, MIPLGP induces an efficient Gaussian processes model with GPU accelerations. Extensive comparative studies validate that existing multi-instance and partial-label algorithms are not able to handle the MIPL problems, and MIPLGP performs significantly better than other algorithms under the MIPL setting. In the future, there are many directions to explore. For example, exploiting the instance-candidate label dependencies or exploring the theoretical properties of MIPL.

References

- [1] Jaume Amores. Multiple instance classification: Review, taxonomy and comparative study. *Artificial Intelligence*, 201:81–105, 2013.
- [2] Lodewijk Brand, Lauren Zoe Baker, Carla Ellefsen, Jackson Sargent, and Hua Wang. A linear primal-dual multi-instance SVM for big data classifications. In *IEEE International Conference on Data Mining, Auckland, New Zealand*, pages 21–30, 2021.
- [3] Forrest Briggs, Xiaoli Z. Fern, and Raviv Raich. Rank-loss support instance machines for MIML instance annotation. In *the 18th ACM SIGKDD International Conference on Knowledge Discovery and Data Mining, Beijing, China*, pages 534–542, 2012.
- [4] Marc-André Carbonneau, Veronika Cheplygina, Eric Granger, and Ghyslain Gagnon. Multiple instance learning: A survey of problem characteristics and applications. *Pattern Recognition*, 77:329–353, 2018.

- [5] Timothee Cour, Ben Sapp, and Ben Taskar. Learning from partial labels. *The Journal of Machine Learning Research*, 12:1501–1536, 2011.
- [6] Lei Feng and Bo An. Partial label learning with self-guided retraining. In *Proceedings of the 33rd AAAI Conference on Artificial Intelligence, Honolulu, Hawaii, USA*, pages 3542–3549, 2019.
- [7] Jacob R. Gardner, Geoff Pleiss, Kilian Q. Weinberger, David Bindel, and Andrew Gordon Wilson. Gpytorch: Blackbox matrix-matrix gaussian process inference with GPU acceleration. In *Advances in Neural Information Processing Systems 31, Montréal, Canada*, pages 7587–7597, 2018.
- [8] Deepti Ghadiyaram, Du Tran, and Dhruv Mahajan. Large-scale weakly-supervised pre-training for video action recognition. In *Proceedings of the 32nd IEEE Conference on Computer Vision and Pattern Recognition, Long Beach, CA, USA*, pages 12046–12055, 2019.
- [9] Chen Gong, Tongliang Liu, Yuanyan Tang, Jian Yang, Jie Yang, and Dacheng Tao. A regularization approach for instance-based superset label learning. *IEEE Transactions on Cybernetics*, 48(3):967–978, 2018.
- [10] Manuel Haußmann, Fred A. Hamprecht, and Melih Kandemir. Variational bayesian multiple instance learning with gaussian processes. In *Proceedings of the 30th IEEE Conference on Computer Vision and Pattern Recognition, Honolulu, HI, USA*, pages 810–819, 2017.
- [11] Eyke Hüllermeier and Jürgen Beringer. Learning from ambiguously labeled examples. *Intelligent Data Analysis*, 10(5):419–439, 2006.
- [12] Maximilian Ilse, Jakub M. Tomczak, and Max Welling. Attention-based deep multiple instance learning. In *Proceedings of the 35th International Conference on Machine Learning, Stockholmsmässan, Stockholm, Sweden*, pages 2132–2141, 2018.
- [13] Rong Jin and Zoubin Ghahramani. Learning with multiple labels. In *Advances in Neural Information Processing Systems 15, Vancouver, British Columbia, Canada*, pages 897–904, 2002.

- [14] Melih Kandemir, Manuel Haußmann, Ferran Diego, Kumar T. Rajamani, Jeroen van der Laak, and Fred A. Hamprecht. Variational weakly supervised gaussian processes. In *Proceedings of the 27th British Machine Vision Conference, York, UK*, pages 71.1–71.12, 2016.
- [15] Minyoung Kim and Fernando De la Torre. Gaussian processes multiple instance learning. In *Proceedings of the 27th International Conference on Machine Learning, Haifa, Israel*, pages 535–542, 2010.
- [16] Diederik P. Kingma and Jimmy Ba. Adam: A method for stochastic optimization. In *Proceedings of the 3rd International Conference on Learning Representations, San Diego, CA, USA*, pages 1–15, 2015.
- [17] Ken Lang. Newsweeder: Learning to filter netnews. In *Proceedings of the 12nd International Conference on Machine Learning, Tahoe City, California, USA*, pages 331–339, 1995.
- [18] Yann LeCun, Léon Bottou, Yoshua Bengio, and Patrick Haffner. Gradient-based learning applied to document recognition. *Proceedings of the IEEE*, 86(11):2278–2324, 1998.
- [19] Liping Liu and Thomas G Dietterich. A conditional multinomial mixture model for superset label learning. In *Advances in Neural Information Processing Systems 25, Cambridge, MA, USA*, pages 548–556, 2012.
- [20] Ilya Loshchilov and Frank Hutter. SGDR: stochastic gradient descent with warm restarts. In *Proceedings of the 5th International Conference on Learning Representations, Toulon, France*, pages 1–16, 2017.
- [21] Jiaqi Lv, Miao Xu, Lei Feng, Gang Niu, Xin Geng, and Masashi Sugiyama. Progressive identification of true labels for partial-label learning. In *Proceedings of the 37th International Conference on Machine Learning, Virtual Event*, pages 6500–6510, 2020.
- [22] Gengyu Lyu, Songhe Feng, Tao Wang, Congyan Lang, and Yidong Li. GM-PLL: Graph matching based partial label learning. *IEEE Transactions on Knowledge and Data Engineering*, 33(2):521–535, 2019.

- [23] Dimitrios Miliotis, Raffaello Camoriano, Pietro Michiardi, Lorenzo Rosasco, and Maurizio Filippone. Dirichlet-based gaussian processes for large-scale calibrated classification. In *Advances in Neural Information Processing Systems 31, Montréal, Canada*, pages 6008–6018, 2018.
- [24] Carl Edward Rasmussen and Christopher K. I. Williams. *Gaussian Processes for Machine Learning*. Cambridge, MA, USA, 2006.
- [25] Burr Settles, Mark Craven, and Soumya Ray. Multiple-instance active learning. In *Advances in Neural Information Processing Systems 20, Vancouver, British Columbia, Canada*, pages 1289–1296, 2007.
- [26] Zhuchen Shao, Hao Bian, Yang Chen, Yifeng Wang, Jian Zhang, Xiangyang Ji, and Yongbing Zhang. Transmil: Transformer based correlated multiple instance learning for whole slide image classification. In *Advances in Neural Information Processing Systems 34, Virtual Event*, pages 2136–2147, 2021.
- [27] Ke Alexander Wang, Geoff Pleiss, Jacob R. Gardner, Stephen Tyree, Kilian Q. Weinberger, and Andrew Gordon Wilson. Exact gaussian processes on a million data points. In *Advances in Neural Information Processing Systems 32, Vancouver, BC, Canada*, pages 14622–14632, 2019.
- [28] Deng-Bao Wang, Min-Ling Zhang, and Li Li. Adaptive graph guided disambiguation for partial label learning. *IEEE Transactions on Pattern Analysis and Machine Intelligence*, 2021.
- [29] Haobo Wang, Ruixuan Xiao, Yixuan Li, Lei Feng, Gang Niu, Gang Chen, and Junbo Zhao. PiCO: Contrastive label disambiguation for partial label learning. In *Proceedings of the 10th International Conference on Learning Representations, Virtual Event*, 2022.
- [30] Yunan Wu, Arne Schmidt, Enrique Hernández-Sánchez, Rafael Molina, and Aggelos K Katsaggelos. Combining attention-based multiple instance learning and gaussian processes for ct hemorrhage detection. In *Proceedings of the 24th International Conference on Medical Image Computing and Computer-Assisted Intervention, Strasbourg, France*, pages 582–591, 2021.

- [31] Han Xiao, Kashif Rasul, and Roland Vollgraf. Fashion-MNIST: a novel image dataset for benchmarking machine learning algorithms. *CoRR*, abs/1708.07747, 2017.
- [32] Zhe Xu, Shaoli Huang, Ya Zhang, and Dacheng Tao. Augmenting strong supervision using web data for fine-grained categorization. In *Proceedings of the IEEE International Conference on Computer Vision, Santiago, Chile*, pages 2524–2532, 2015.
- [33] Yu-Yan Xu, Yang Shen, Xiu-Shen Wei, and Jian Yang. Webly-supervised fine-grained recognition with partial label learning. In *Proceedings of the 31st International Joint Conference on Artificial Intelligence, Virtual Event / Vienna, Austria*, pages 1502–1508, 2022.
- [34] Fei Yu and Min-Ling Zhang. Maximum margin partial label learning. *Machine Learning*, 4(106):573–593, 2016.
- [35] Hongrun Zhang, Yanda Meng, Yitian Zhao, Yihong Qiao, Xiaoyun Yang, Sarah E Coupland, and Yalin Zheng. DTFD-MIL: Double-tier feature distillation multiple instance learning for histopathology whole slide image classification. In *Proceedings of the 35th IEEE Conference on Computer Vision and Pattern Recognition, New Orleans, USA*, pages 18802–18812, 2022.
- [36] Weijia Zhang, Xuanhui Zhang, Han-Wen Deng, and Min-Ling Zhang. Multi-instance causal representation learning for instance label prediction and out-of-distribution generalization. In *Advances in Neural Information Processing Systems 35, New Orleans, USA*, pages 1–13, 2022.
- [37] Weijia Zhang. Non-I.I.D. multi-instance learning for predicting instance and bag labels with variational auto-encoder. In *Proceedings of the 30th Thirtieth International Joint Conference on Artificial Intelligence, Virtual Event / Montreal, Canada*, pages 3377–3383, 2021.
- [38] Zhi-Hua Zhou and Min-Ling Zhang. Multi-instance multi-label learning with application to scene classification. In *Advances in Neural Information Processing Systems 19, Vancouver, British Columbia, Canada*, pages 1609–1616, 2006.

- [39] Yu Zhou, Jianjun He, and Hong Gu. Partial label learning via gaussian processes. *IEEE Transactions on Cybernetics*, 47(12):4443–4450, 2016.
- [40] Zhi-Hua Zhou. A brief introduction to weakly supervised learning. *National Science Review*, 5(1):44–53, 2018.

Appendix A. The MIPL Datasets

In this section, we provide the details of the MIPL datasets, i.e., MNIST-MIPL, FMNIST-MIPL, Newsgroups-MIPL, Birdsong-MIPL, and SIVAL-MIPL.

For MNIST-MIPL, FMNIST-MIPL, and Newsgroups-MIPL datasets, we need to choose the targeted class labels and the reserved class labels to provide each multi-instance bag with positive instances and negative ones. For MNIST-MIPL dataset, we extract $\{0, 2, 4, 6, 8\}$ as five target classes for providing the positive instances according to the corresponding class and draw all negative ones from the reserved classes $\{1, 3, 5, 7, 9\}$ randomly. For FMNIST-MIPL dataset, the targeted class labels and the reserved class labels are $\{T\text{-shirt}, T\text{rouser}, C\text{coat}, S\text{neaker}, B\text{ag}\}$ and $\{P\text{ullover}, D\text{ress}, S\text{andal}, S\text{hirt}, A\text{nkle boot}\}$, respectively. Newsgroups-MIPL, the dataset is widely used in binary multi-instance learning, where each instance is represented by the top 200 TF-IDF features, and each positive bag contains 3% positive instances drawn from the target class. Similarly, we represent each instance by the top 200 TF-IDF features in Newsgroups-MIPL, and Table 5 summarizes the targeted class labels and the reserved class labels of Newsgroups-MIPL dataset.

The Birdsong dataset is proposed in multi-instance multi-label learning, which contains 548 multi-instance bags totalling 10232 instances. Each instance is represented by a 38-dimensional feature vector and associated with a single label, which is chosen from 13 targeted class labels or 1 negative class label. In Birdsong-MIPL, the 13 targeted class labels

Table 5: The targeted class labels and reserved class labels of Newsgroups-MIPL dataset.

Targeted class labels	Reserved class labels
alt.atheism	comp.graphics
comp.os.ms-windows.misc	comp.sys.ibm.pc.hardware
comp.sys.mac.hardware	comp.windows.x
misc.forsale	rec.motorcycles
rec.autos	rec.sport.baseball
rec.sport.hockey	sci.crypt
sci.med	sci.electronics
sci.space	talk.politics.guns
soc.religion.christian	talk.politics.misc
talk.politics.mideast	talk.religion.misc

and the negative class label are regarded as the targeted class labels and the reserved class label, respectively.

SIVAL is a multi-instance learning dataset for content-based image retrieval with 1500 images. Each image is a multi-instance bag, which is associated with one of 25 class labels and consisted of 31 or 32 instances. In addition, each instance is represented by a 30-dimensional feature vector. To yield the SIVAL-MIPL, we only need to generate the false positive labels for each image. Specifically, we treat the 25 class labels as the targeted class labels and sample r false positive labels from the targeted class labels excluding the ground-truth label randomly.